

PID CONTROLLER FOR UNMANNED AERIAL VEHICLE IN CLOSED ENVIRONMENT USING FIDUCIAL MARKER SYSTEMS

M.S. Amiri^{1*}, R. Ramli², I.E. Zaidi² and M. Van³

¹Fakulti Teknologi dan Kejuruteraan Industri dan Pembuatan,
Universiti Teknikal Malaysia Melaka,
76100 Durian Tunggal, Melaka, Malaysia.

²Faculty of Engineering and Built Environment,
Universiti Kebangsaan Malaysia,
43600 Bangi, Selangor, Malaysia.

³School of Electronics, Electrical Engineering and Computer Science,
Queen's University Belfast,
BT9 5BN Belfast, United Kingdom

*Corresponding Author's Email: soleimani@utem.edu.my

Article History: Received 26 January 2024; Revised 7 July 2024; Accepted 20 July 2024

©2024 M.S.. Amiri et al. Published by Penerbit Universiti Teknikal Malaysia Melaka. This is an open article under the CC-BY-NC-ND license (<https://creativecommons.org/licenses/by-nc-nd/4.0/>).

ABSTRACT: Unmanned Aerial Vehicles (UAVs) are widely used for various purposes, including surveillance, inspection, supply delivery, and military operations. The conventional navigation technologies have deficits in accuracy and robustness in narrowed environments and do not properly support fully autonomous robotic functionalities. The aim of this paper is to develop an autonomous navigation algorithm for a UAV using a tag-based visual system. In this paper, a navigation method based on fiducial marker systems has been established. A Proportional-Integral-Derivative (PID) controller has been established to track the UAV toward the desired path. The navigation algorithm has been programmed in Python and the Robot Operating System (ROS) and implemented in a DJI Tello as an UAV application. An experimental set has been provided to validate the navigation performance. The average error of the proposed navigation system is 0.19, 0.08, and 0.83 radian in X, Y, and Z axes. The experimental results showed the efficiency and stability of the developed autonomous navigation algorithm for

UAVs using the Apriltag visual system along with the PID controller. As future work, the proposed navigation system will be improved to incorporate obstacle avoidance capabilities and enhanced multi-UAV coordination in more complex environments.

KEYWORDS: *Autonomous Navigation; unmanned aerial vehicle; AprilTag, PID controller; Fiducial marker systems*

1.0 INTRODUCTION

An Unmanned Aerial Vehicle (UAV) is a type of remotely operated or autonomous aircraft used for various purposes, including surveillance, mapping, inspection, delivery, and even military operations[1]. UAVs come in various sizes, ranging from small and light to large and heavy, and can be powered by different methods, including electric motors, combustion engines, or even solar panels [2]. Equipped with a variety of sensors and cameras, they capture images and data from the air and can be controlled remotely using radio or satellite links [3].

One of the primary reasons for the extensive use of UAVs is their capability to navigate areas deemed unsafe for human entry [4]. Infrastructure, such as buildings, bridges, and oil and gas refineries, necessitates regular and comprehensive inspections. However, conducting these inspections presents challenges, including the sheer size of structures, limited accessibility, the risk of accidents for inspectors, and various other factors. Consequently, many companies find investing in UAVs to be an alternative solution to effectively address these challenges [5].

Autonomous navigation encompasses various tasks, including localization, scenario mapping, route planning, and obstacle avoidance. In outdoor environments, localization and tracking can be accomplished using a Global Positioning System (GPS). Conversely, in indoor settings, such an approach becomes impractical as the signal is obstructed by buildings, rendering GPS-based UAV localization unfeasible due to the absence of a signal inside a building [6].

One of the primary challenges is to devise efficient algorithms that enable UAVs to safely navigate indoor environments. These algorithms must take into account both static and dynamic obstacles, requiring a comprehensive understanding of the UAV's surrounding environment for successful autonomous navigation [7]. Indoor environments, being

semi-enclosed spaces, often pose constraints on flight due to limited space compared to outdoor settings. These spaces are typically small, featuring narrow passages with various obstacles that pose challenges for UAV navigation [8]. Hence, precise navigation and stable flight are essential to prevent collisions with ceilings, walls, and other obstacles. Selma et al. [9] presented a novel tracking system utilizing a hybrid controller that combines a robust adaptive neuro-fuzzy inference system with a particle swarm optimization algorithm for navigation.

For localization and navigation in closed environments, various methods have been explored, including vision-based models that utilize different techniques such as visual odometry and Simultaneous Mapping and Localization (SLAM) [10]. The drawback of employing these two systems is the high computational load. However, they are not suitable for the scope of this project. Therefore, there is a need for low-cost, easy-to-install, and high-performance systems for autonomous navigation of air vehicles in closed environments [11].

Fiducial markers are commonly employed in object manipulation tasks, where graphical markers play a key role in recognizing, detecting, and localizing various objects [12]. These graphical markers are specifically designed for use on flat surfaces, such as walls. Each marker possesses its own identity and corresponding graphical representation, recognized by computer vision algorithms. Fiducial markers like AprilTag are commonly employed in indoor navigation due to their cost-effectiveness and lower processing power requirements.

In some studies, the Proportional-Integral-Derivative (PID) controller is utilized to guide the UAV along a specific trajectory. Li et al. [13] studied the accuracy of PID control to enhance the position tracking and landing of UAVs, employing AprilTag as a ground marker. The findings indicated that maintaining an offset between the landing ground and AprilTag resulted in a favourable tracking effect. Moreover, the markers improved accuracy and robustness by offering recognizable features crucial for UAV navigation in indoor environments [14]. This paper employs the AprilTag visual system to develop an autonomous navigation algorithm in an indoor environment.

From mentioned research, the conventional navigation system based on SLAM have issues in accuracy and robustness in indoor area especially in the narrowed environment. The objective of this paper is

to develop an accurate navigation system of UAV by using image processing application. This research aims to enhance autonomous indoor flight by improving the stability of the UAV through the implementation of an autonomous movement algorithm. The novelty and significant of this work are to develop a navigation method to address the accuracy issue of navigation system based on integration of AprilTag and PID controller.

The remainder of this paper is structured as follows: Section 2 discusses the visual-based navigation of the developed UAV, while Section 3 presents the results and discussion. Finally, Section 4 provides the conclusion of this paper.

2.0 UAV VISUAL-BASED NAVIGATION DEVELOPMENT

2.1 UAV Hardware structure

The drone used in this study, manufactured by DJI and called Tello, offers an Application Programming Interface (API) that supports communication and control of the UAV through programming. The use of WiFi for communication allows remote interaction with the UAV, enabling a wide array of applications and functionalities [15].

The DJI Tello features an Inertial Measurement Unit (IMU) that contributes to stability and precision during flight, ensuring reliable data collection and precise control responses. Moreover, the Tello UAV's 720p camera is well-suited for AprilTag detection. The rotational velocity of the UAV is measured through angular rates, as illustrated in Figure 1 [16].

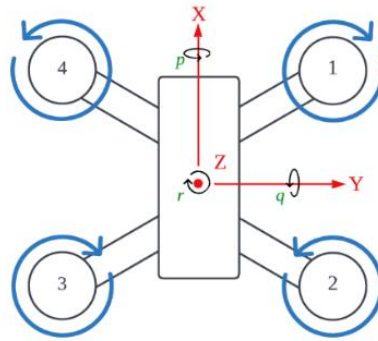


Figure 1: A quadcopter body-fixed coordinate system.

In Figure 1, p is rotation around the X axis, q is around the Y axis, and r is rotation around the Z axis. To relate the orientation of the local coordinate system relative to a global one, the Euler angles roll, pitch, and yaw are used. This coordinate system is commonly employed in aeronautical applications to describe and relate the orientation, motion, and measurements of aircraft. A quadcopter is a type of UAV that typically comprises four motors and rotors. One frequently used configuration involves two motors spinning in a clockwise direction and the other two spinning counterclockwise. This arrangement facilitates the manipulation of the quadcopter's roll, pitch, and yaw angles by having the diagonal motors rotate in sync.

2.2 AprilTag-Based Navigation method

The AprilTag visual system comprises two primary components: a labelling detector and a coding system [17]. The detector's role is to determine the relative position and orientation of an AprilTag from a camera. Meanwhile, the coding system is employed to retrieve the data encoded within AprilTags [18]. The positioning process involves two main stages: first, the detection of the tag itself, and second, the estimation of its orientation [19]. Figure 2 illustrates the process of AprilTag detection.

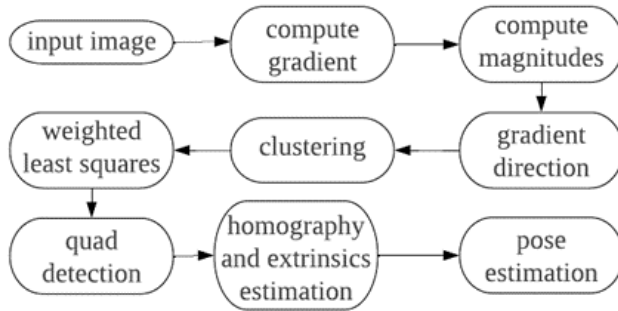


Figure 2: The process of AprilTag detection and pose estimation.

The orientation of the AprilTag center can be determined in three dimensions based on the camera view, which is then used as the position control input in the PID controller. Figure 3 illustrates the UAV positioning in relation to the position of the AprilTag marker.

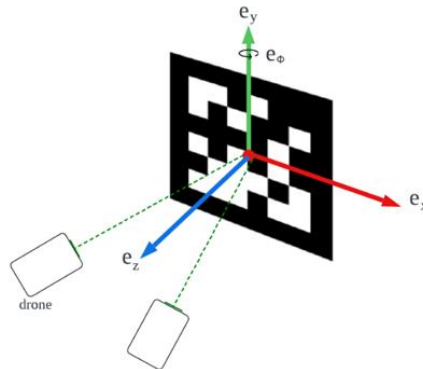


Figure 3: Drone navigation based on Tag Marker

The PID controller has been employed as a widely used feedback control system in engineering applications for regulating the output of the system [20]. The PID controller is utilized to autonomously manoeuvre the UAV based on the orientation and position of the AprilTag relative to the body frame [21]. Figure 4 illustrates the diagram of the PID controller.

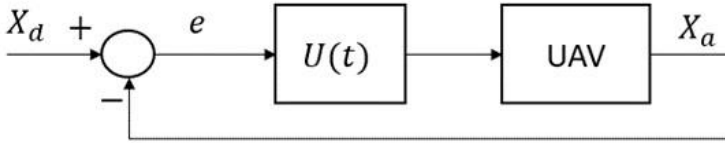


Figure 4: PID Controller diagram

The output of the PID is the velocity of the body frame, which is influenced by proportion, integral, and derivative of the steady-state error. The equation of PID controller is given as follows:

$$u(t) = K_p e + K_i \int e dt + K_d \frac{de}{dt} \tag{1}$$

where $u(t)$ is the equation of the PID controller in time domain. In this study, an iterative adjustment method to fine-tune the PID controller has been employed. In this equation, K_p , K_i , and K_d are proportional, integral and derivative coefficients. The steady-state error is then determined as the difference between the actual and desired positions of the UAV, given as follows:

$$e = X_d - X_a \tag{2}$$

Where $e = [e_x \ e_y \ e_z \ e_\psi]^T$ is the steady state error, $X_d = [x_d \ y_d \ z_d \ \psi_d]^T$ is the desired position, and $X_a = [x_a \ y_a \ z_a \ \psi_a]^T$ is the actual position. In addition, e_x , e_y , e_z , and e_ψ are the steady-state error in x , y , z , and yaw directions, respectively. Furthermore, x_d , y_d , z_d , and ψ_d are the desired position of the UAV in x , y , z , and yaw directions, respectively. Moreover, x_a , y_a , z_a , and ψ_a are the actual position of the UAV in x , y , z , and yaw directions, respectively.

This method involves a systematic process of adjusting the proportional, integral, and derivative gains to achieve satisfactory control performance and minimize errors between the desired and actual outputs.

The PID controller receives pose estimation data from an AprilTag captured by the camera. As the UAV's speed is directly linked to the position offset, the difference between the UAV and the tag's position is utilized as the input speed for the UAV.

Through the adjustment of these parameters, the PID controller regulates the motor commands of the UAV, correcting its movement. As the UAV's state converges toward the desired state, the PID controller reduces corrective actions to prevent overshooting or instability. This iterative process persists, ensuring that the UAV progressively converges towards and sustains its desired pose relative to the AprilTag. Navigating of the UAV have been developed in the Robot Operating System (ROS), which is a platform to provide libraries to build a robot application. In this paper, ROS is used to implement the navigation into the UAV and communicate with it through WiFi. The navigation system is programmed in Python and controlled velocity, that conducted by PID controller transferred to UAV by ROS nodes [22]. Figure 5 depicts the communication framework of the system employing ROS.

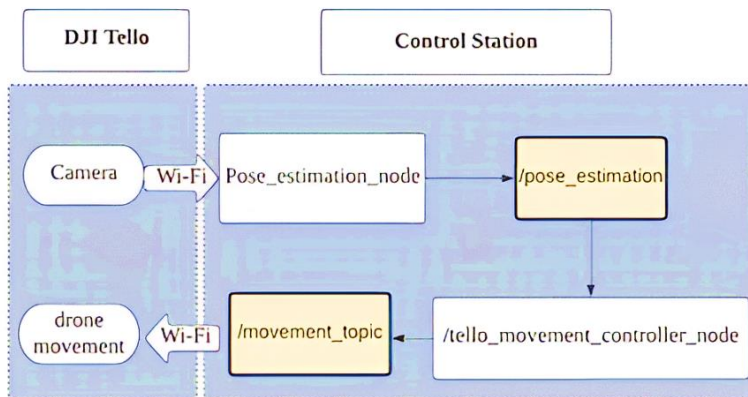


Figure 5: Communication between UAV and control station.

The UAV control station communicates via Wi-Fi. The navigation algorithm, developed in Python, operates on a PC functioning as the control station. The UAV's camera publishes an image that is subscribed to by the pose_estimation_node. Within this node, AprilTag detection takes place, and pose estimation for all four axes is derived. The collected data is stored throughout the flight for subsequent analysis. After acquiring pose estimation data, the node publishes a topic containing this data to the tello_movement_controller_node. Within this node, PID calculations are performed to determine the output velocity, which is then transmitted back to the DJI Tello drone via a movement topic. Communication between the UAV and the ground station is maintained continuously throughout the UAV's

flight.

The scenario of navigation algorithm is divided into four stages. Firstly, the control system is applied to uplift the drone upward, z-axis. After the drone reached certain desired height, it rotated in yaw angle until desired tolerance error range is obtained. Then it moved to its side direction of Y-axis. The last stage is forward direction, X-axis. Whenever the drone carries out the defined tolerance in all the stages, the drone will be in desired position [23]. Algorithm 1 shows the pseudo-code outlining the scenario of the navigation system, with μ representing the error tolerance.

Algorithm 1. Pseudo-code of navigation algorithm.

1. Start
 2. Take off
 3. Navigate in Z-axis
 4. If $e_z < \mu_z$:
 5. Navigate in yaw-axis
 6. If $e_z < \mu_z$ & $e_\psi < \mu_\psi$:
 7. Navigate in Y-axis
 8. If $e_z < \mu_z$ & $e_\psi < \mu_\psi$ & $e_y < \mu_y$:
 9. Navigate in X-axis
 10. If $e_z < \mu_z$ & $e_\psi < \mu_\psi$ & $e_y < \mu_y$ & $e_x < \mu_x$
 11. Land
 12. End
-

In the scenario of the navigation system, the trajectory is presented to lead the drone to reach its target point. Therefore, a desired path trajectory to the target can be predicted to avoid potential crashes. Figure 6 represents the flowchart of the navigation system.

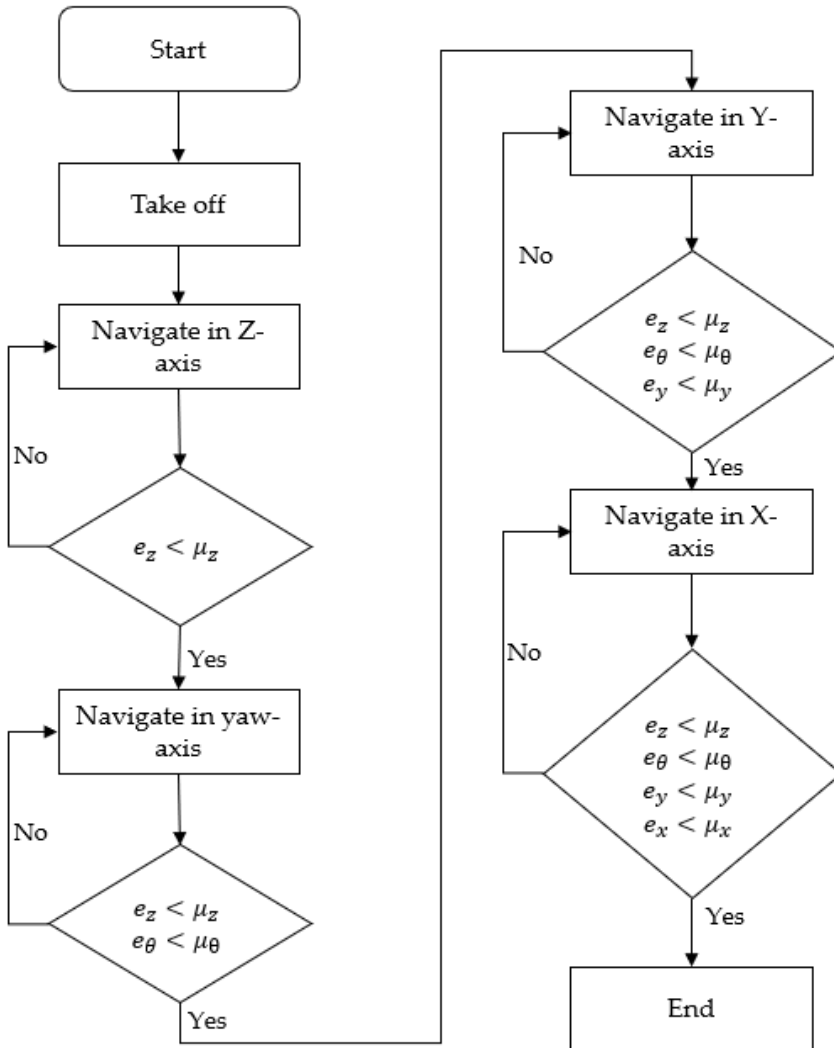


Figure 6: Flowchart of the navigation algorithm.

The conventional navigation methods used map and laser sensor to navigate the UAV, but in the proposed method the image processing is used for navigation. The proposed navigation method in Algorithm 1 has four stages to validate the steady-state error, confirming the accuracy and robustness of the navigation system. Moreover, in this method, a pre-defined map for the navigating environment is not required. This increases the accuracy in navigation specially for the narrowed places.

3.0 RESULTS AND DISCUSSION

In this study, an experiment to evaluate the tag-based navigation system has been conducted. Figure 7 represents the experimental platform using a Tello as an UAV.



Figure 7: Experimental platform for UAV navigation.

To simulate the narrow and enclosed conditions in an indoor area, three obstacles were built for the drone to pass through the obstacles without colliding. The top of each stand frame is square-shaped, measuring 25cm x 25cm, and has a total height of 125cm, as shown in Figure 7. An AprilTag is placed in the middle of each frame. The UAV navigated through the square-shaped frames and landed after passing the last one.

The stand frames were positioned at 90 degrees to each other. After adjusting the distance of UAV and AprilTag in each stand, the UAV passes through each square-shape frame. This trend repeats for frame 1, frame 2, and frame 3. Figure 8 illustrates the schematic of the navigation.

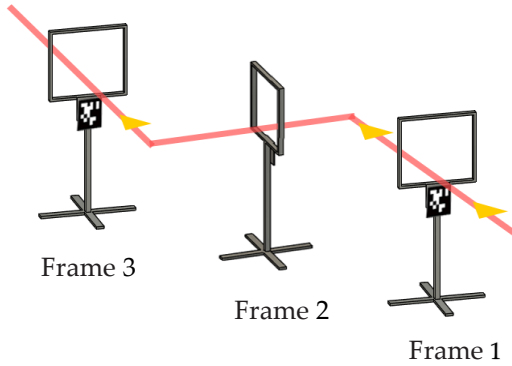


Figure 8: Schematic UAV path for the experiment.

Firstly, the control system is applied to lift the UAV upward in the Z-axis. Once it reaches the desired height, it rotates at a yaw angle and in the Y-axis simultaneously until the desired tolerance error range is achieved. Subsequently, it moves forward to approach the AprilTag located in the middle of the obstacle. After the UAV is within the tolerance error range of the X-axis, it aligns the Y-axis, yaw axis, and the Z-axis to ensure that it is in the desired position. Upon achieving the defined tolerance, the UAV then ascends and passes through the obstacle. Finally, it rotates 90 degrees, ready for the next obstacle, running the same code loop. Table 1 represents parameters of PID for each axis in detail.

Table 1: PID controller parameters

Axis	Setpoint	K_p	K_i	K_d
X	0.0 m	0.6	0.01	0.01
Y	0.0 m	2	0.01	0.1
Z	0.45 m	1.3	0	0.1
Yaw	0 rad	0.2	0	0.1

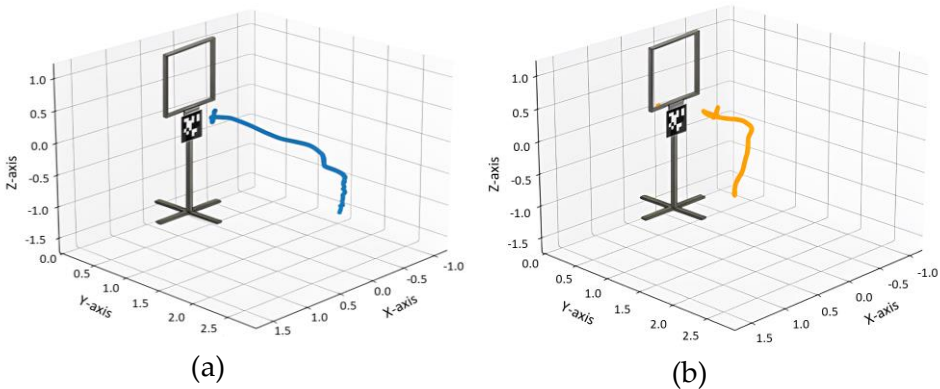
The setpoints are selected based on the structure of the experimental platform to avoid possible collision between UAV and the frames. The setpoints for x and y are set as zero, representing the centre of square-shaped frame and setpoint of z shows the distance of the drone to the frames. The parameters of PID controller are selected based on oscillation observing method.

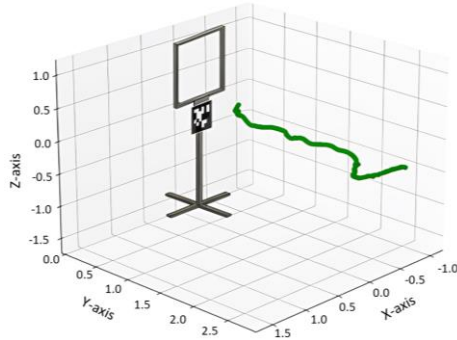
Theoretically the tuning process starts to avoid instability, involving a gradual increment of the proportional gain for quicker responsiveness and reduce oscillations. When oscillations occur, a small derivative

gain is set to smooth out the response. The integral gain is then added to correct any lingering errors. Through adjustment of PID parameters and performance evaluation by oscillation observing method, the tuned values can be achieved to balance between accuracy and stability in controlling the UAV's movements.

The setpoints for each axis represent the desired distances relative to the AprilTag axis, as depicted in Figure 7. Specifically, the setpoints for X and Y axes are both set to 0 m, measured from the centre of the tag. For the Z-axis, the setpoint is 0.45 m, representing the desired distance between the UAV and the AprilTag. Finally, the setpoint for the Yaw axis is defined as zero, ensuring the UAV is perpendicular to the AprilTag. To maintain stability during flight, lower and upper limits are set to control the speed within an appropriate range.

During the experiment, the UAV has been flown through the provided frames to validate the proposed navigation system. The UAV position regarding the tag images has been measured and transferred to the ground station through ROS and WiFi. Figure 8 represents the UAV trajectory flying to the frames in 3-dimensions.

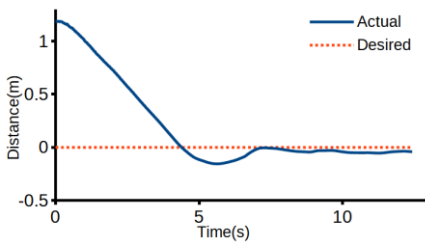




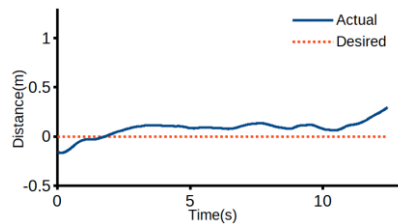
(c)

Figure 9: Trajectory tracking of UAV flying toward the stand frame.
 (a) Standing frame 1 (b) Standing frame 2 (c) Standing frame 3 in meter.

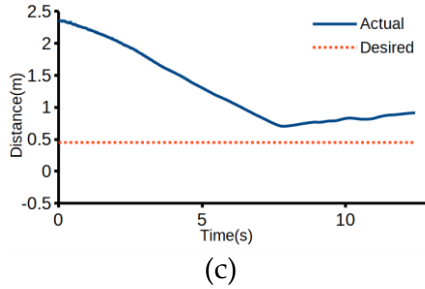
These trajectories are distance of the camera frame regarding the AprilTag located on the standing frames in 3- dimensional. The sequence of the navigation is frame 1, frame 2, and frame 3 as represented in Figure 8. Therefore, trajectory of UAV moving toward the first frame is represented in Figure 9(a). After the UAV accomplished its navigation toward AprilTag, it passed the first square-shaped frame, which is represented in Figure 9(b). Similarly, the UAV flew toward the third frame, after fulfilling the navigation of Frame 2, as shown in Figure 9(c). As can be seen, in Figure 9, UAV manoeuvred toward the provided frames and reached to the destination based on the navigation algorithm mentioned in Algorithm 1. For further discussion, Figure 10 represents the UAV trajectories in x, y, z, and yaw directions toward the first standing frame.



(a)



(b)



(c)
 Figure 10: UAV trajectory tracking (a) X-axis (b) Y-axis (c) Z-axis for standing frame 1.

In Figure 10, the X-axis, Y-axis and Z-axis are regarding to the camera and tag-marker, in which the desired trajectories are set 0, 0, and 0.45 meter. The actual trajectory follows the desired path gradually. This result reveals that in the navigation algorithm, PID controller leads the UAV to move toward the desired trajectories. Therefore, the algorithm worked efficiently and has a significant performance to navigate the UAV to the desired point.

In Figure 10(a), there is a decrease from a distance of 1.2 meters relative to the AprilTag. This is because the UAV is not directly opposite the AprilTag, unlike in the first obstacle. The UAV successfully adjusted its position to the setpoint, with only a slight drift recorded. Subsequently, the UAV maintains a stable flight on the X-axis relative to the AprilTag. Figure 10(b) shows an increase from a distance of -0.15 meters relative to the AprilTag. This occurs as the UAV descends slightly after passing the first obstacle on the Y-axis. Although the UAV returns to the setpoint position, it records a significant error of up to 0.1 meters higher than the AprilTag. For Figure 10(c), which represents the Z-axis PID control, the data exhibits stable PID control and constant velocity movement until reaching the setpoint opposite the tag. However, compared to the previous figure, the UAV produces a relatively large error after reaching the setpoint before proceeding to the next operation. It can be obtained from the figures, that the PID adjusted the position smoothly at the beginning and gradually the actual follows desired trajectory.

In an efficient control system, the actual should follows the desired trajectory. In Figure 10, the UAV moved toward the defined desired position. The average error of X-axis, Y-axis, and Z-axis are 0.19, 0.08, and 0.83 radian that represents the efficiency of the navigation system, although there is an obvious steady-state error in X-axis. The difference in average error among different directions navigation is related to the

PID parameters mentioned in Table 1 and distance of the starting location of the UAV and the desired position. These results approved the values determined in Table 1 able to navigate the UAV in the defined experimental platform without collision with obstacles.

In general, it can be observed that the proposed navigation method performed efficiently based on the AprilTag as the image processing application and PID controller for tracking the actual trajectory created by the AprilTag distance measurement. From the experimental results, the efficiency and stability of the UAV autonomous navigation algorithm using the AprilTag visual system along with the PID controller are concluded [21].

4.0 CONCLUSION

This paper aimed to evaluate the feasibility of using UAVs for navigation in indoor environments by employing the AprilTag system for UAV localization. The implementation of the PID controller demonstrated the UAV's stability during flight, successfully navigating through a series of built obstacles. AprilTag's robust tracking ability and accurate localization information allowed the UAV to maintain a stable flight path, avoiding potential collisions with obstacles. The PID controller played a crucial role in enhancing the stability and control of the UAV during flight. Its continuous adjustment of the UAV's control inputs based on error inputs contributed to a more stable flight trajectory, facilitating smoother navigation across obstacle courses.

Furthermore, this paper demonstrates the enhanced potential of utilizing UAVs with AprilTag-based localization and PID control for precise navigation through obstacles. The system exhibits high accuracy, making it suitable for various applications, particularly in confined spaces like indoor areas. However, challenges encountered during UAV flight, such as inconsistent PID control, that are highlighted in this study. Future investigations could explore the integration of fuzzy and adaptive control systems for visual-based navigation to potentially overcome these challenges. In addition, the proposed method will be improved to incorporate obstacle avoidance capabilities and enhanced multi-UAV coordination in more complex environments.

ACKNOWLEDGMENTS

The authors would like to thank Universiti Teknikal Malaysia Melaka (UTeM) and Universiti Kebangsaan Malaysia (UKM) for their support in conducting this research.

AUTHOR CONTRIBUTIONS

MSA: Conceptualization, Methodology, Software, Writing- Original Draft Preparation; RR: Data Curation, Validation, Supervision; IEZ: Software, Validation; MV: Writing-Reviewing and Editing.

CONFLICTS OF INTEREST

The manuscript has not been published elsewhere and is not under consideration by other journals. All authors have approved the review, agree with its submission and declare no conflict of interest on the manuscript.

REFERENCES

- [1] A.S.M. Yazid, R.A. Wahid, K.M. Nazrin, A. Ahmad, A.S. Nasruddin, D. Rozilawati, M.A. Hamzah and M.Y.A. Razak, "Terrain Mapping from Unmanned Aerial Vehicles", *Journal of Advanced Manufacturing Technology*, vol. 13, no. 1, pp. 1–16, 2019.
- [2] M. Emimi, M. Khaleel, and A. Alkrash, "The Current Opportunities and Challenges in Drone Technology", *International Journal of Electrical Engineering and Sustainability*, vol. 1, no. 3, pp. 74–89, 2023.
- [3] A. R. Merheb, H. Noura, and F. Bateman, "Emergency control of AR drone quadrotor UAV suffering a total loss of one rotor", *IEEE/ASME Transactions on Mechatronics*, vol. 22, no. 2, pp. 961–971, 2017.
- [4] M. M. Quamar, B. Al-Ramadan, K. Khan, M. Shafiullah, and S. El Ferik, "Advancements and Applications of Drone-Integrated Geographic Information System Technology – A Review", *Remote Sensing*, vol. 15, no. 20, pp. 5039-5074, 2023.
- [5] P. Nooralishahi, C. Ibarra-Castanedo, S. Deane, F. López, S. Pant, N. Genest, N.P. Avdelidis and X.P.V. Maldague, "Drone-based non-destructive inspection of industrial sites: A review and case studies", *Drones*, vol. 5, no. 4, pp. 106-135, 2021.
- [6] S. W. Loke, "Enabling Drone Services: Drone Crowdsourcing and

- Drone Scripting”, *IEEE Access*, vol. 7, pp. 110035–110049, 2019.
- [7] Y. Khosiawan, Y. Park, I. Moon, J. M. Nilakantan, and I. Nielsen, “Task scheduling system for UAV operations in indoor environment,” *Neural Computing and Applications*, vol. 31, no. 9, pp. 5431–5459, 2019.
- [8] M. Nahangi, A. Heins, B. McCabe, and A. Schoellig, “Automated Localization of UAVs in GPS-Denied Indoor Construction Environments Using Fiducial Markers”, *35th International Symposium on Automation and Robotics in Construction (ISARC 2018)*, Berlin, Germany, pp. 88-94, 2018.
- [9] B. Selma, S. Chouraqui, and H. Abouaïssa, “Fuzzy swarm trajectory tracking control of unmanned aerial vehicle”, *Journal of Computational Design and Engineering*, vol. 7, no. 4, pp. 435–447, 2020.
- [10] A. Famili and J.-M. Park, “ROLATIN: Robust Localization and Tracking for Indoor Navigation of Drones”, *IEEE Wireless Communications and Networking Conference (WCNC)*, Seoul, Korea (South), pp. 1-6, 2020.
- [11] N. Gageik, M. Strohmeier, and S. Montenegro, “An autonomous UAV with an optical flow sensor for positioning and navigation”, *International Journal of Advanced Robotic Systems*, vol. 10, no. 10, pp. 1-9, 2013.
- [12] A. Sagitov, K. Shabalina, R. Lavrenov, and E. Magid, “Comparing fiducial marker systems in the presence of occlusion”, *2017 International Conference on Mechanical, System and Control Engineering, ICMSC 2017*, pp. 377–382, 2017.
- [13] Z. Li, Y. Chen, H. Lu, H. Wu, and L. Cheng, “UAV Autonomous Landing Technology Based on AprilTags Vision Positioning Algorithm”, *Proceedings of the 38th Chinese Control Conference*, Guangzhou, China, pp. 8148-8153, 2019.
- [14] M. Kalaitzakis, B. Cain, S. Carroll, A. Ambrosi, C. Whitehead, and N. Vitzilaios, “Fiducial Markers for Pose Estimation”, *Journal of Intelligent & Robotic Systems*, vol. 101, no. 71, pp. 1-26, 2021.
- [15] M. Pawlicki, K. Hulek, A. Ostrowski, and J. Możaryn, “Implementation and analysis of Ryze Tello drone vision-based positioning using AprilTags”, *27th International Conference on Methods and Models in Automation and Robotics (MMAR)*, Międzyzdroje, Poland, pp. 309–313, 2023.
- [16] A. Mughees and I. Ahmad, “Multi-Optimization of Novel Conditioned Adaptive Barrier Function Integral Terminal SMC for Trajectory Tracking of a Quadcopter System”, *IEEE Access*, vol. 11, pp. 88359–88377, 2023.
- [17] J. Chen, Y. Gao, and S. Li, “Real-time Apriltag Inertial Fusion Localization for Large Indoor Navigation”, *Proceedings - 2020 Chinese*

- Automation Congress (CAC)*, Shanghai, China, pp. 6912–6916, 2020.
- [18] D. Malyuta, C. Brommer, D. Hentzen, T. Stastny, R. Siegwart, and R. Brockers, “Long-duration fully autonomous operation of rotorcraft unmanned aerial systems for remote-sensing data acquisition”, *Journal of Field Robotics*, vol. 37, no. 1, pp. 137–157, 2020.
- [19] M. Farris Khyasudeen, M. Badri, M. Noor, S. R. Azzuhri, and N. Buniyamin, “Computers and Informatics Unmanned aerial vehicles precision landing on a moving platform using image matrix segmentation method”, *Computers and Informatics*, vol. 4, no. 1, pp. 1-12, 2024.
- [20] A. M. Abdullah, R. M. Ridzuan, F. Ahmad, F. Mohamed Jamil and M. Ibrahim, “Vehicle Active Suspension Control Using Multi-Order Pid Approach”, *Journal of Advanced Manufacturing Technology*, vol. 11, no. 1, pp. 1–14, 2017.
- [21] M. S. Amiri and R. Ramli, “Visual Navigation System for Autonomous Drone using Fiducial Marker Detection”, *International Journal of Advanced Computer Science and Applications*, vol. 13, no. 9, pp. 683-690, 2022.
- [22] K.-L. Chang and H.-Y. Lin, “System Development and Integration of Unmanned Aerial Vehicle Navigation Techniques for Indoor Environments”, *IEEE International Conference on Industrial Technology (ICIT)*, Bristol, United Kingdom, pp. 1–6, 2024.
- [23] M. S. Amiri, R. Ramli, and A. H. Faizal, “Simultaneous Localization and Mapping and Tag-Based Navigation for Unmanned Aerial Vehicles”, *International Journal of Integrated Engineering*, vol. 15, no. 5, pp. 225-232, 2023.

